Facile synthesis and application of highly luminescent CdTe quantum dots with an electrogenerated precursor†

Cunwang Ge,[ab] Min Xu,[a] Jing Liu,[b] Jianping Lei[a] and Huangxian Ju*[a]

Received (in Cambridge, UK) 1st October 2007, Accepted 5th November 2007
First published as an Advance Article on the web 13th November 2007
DOI: 10.1039/b714990e

An electrogenerated precursor has been developed for green synthesis of highly luminescent aqueous CdTe quantum dots (QDs) with unique quantum yield and strong electrogenerated luminescence, which can access cellular targets *via* specific binding and have potential application as biolabels in highly sensitive biosensing and cell imaging.

CdTe quantum dots (QDs) are currently attracting enthusiastic interest due to their unique size-dependent optical and electrical properties for potential application in optoelectronics and biolabeling. However, the low quantum yield (QY) and difficult synthesis of aqueous CdTe QDs are hindering their application in biological imaging[1a] and detection.[1b] Up to now three types of tellurium sources, Te powders,[2,3] Al_2Te_3 lumps[4] and TeO_3^{2-},[5,6] have been used for the synthesis of CdTe. Te powders, the most popular source, must first be dissolved in high-boiling-point solvents for nonaqueous synthesis,[2] or slowly reduced by $NaBH_4$ to NaHTe[3a,b] or reacted with ammonia and aluminium to give $(NH_4)_2Te$[3c] for aqueous synthesis under an inert atmosphere. When humidity-sensitive Al_2Te_3 lumps are used as a source of NaHTe, the synthesis has to be performed with a Schlenk line.[2,4] Although TeO_3^{2-} as an alternative Te source can be reduced for preparing CdTe film[5] or nanowire arrays[6] by electrodeposition of self-controlled atomic layer epitaxy, the products cannot be converted to luminescent CdTe QDs.

Herein, we report a facile synthesis of highly luminescent CdTe QDs in an aqueous system with a novel Te source to conveniently produce a CdTe precursor using a cathodic stripping Te electrode. The versatility of the present protocol has been validated by preparing CdTe QDs with different functional groups using mercaptoacetic acid (MAA) and *N*-acetylcysteine (ACYS) as stabilizers. The luminescent behaviors of as-prepared QDs investigated by photoluminescence (PL) and electrogenerated luminescence (ECL) show their potential application in optical and ECL biosensing with high sensitivity. The as-prepared CdTe QDs were successfully labeled to antibody for access to cellular targets for cell imaging.

[a]*Key Laboratory of Analytical Chemistry for Life Science (Education Ministry of China), Department of Chemistry, Nanjing University, Nanjing 210093, P. R. China. E-mail: hxju@ nju.edu.cn; Fax: +86-25-83593593; Tel: +86-25-83593593*
[b]*Department of Chemistry, Nantong University, Nantong 226007, P. R. China*

† Electronic supplementary information (ESI) available: Related reagents, instrumentation, electrochemistry of Cd^{2+} with MAA, schematic depiction of synthesis of CdTe QDs, effect of molar ratio of Cd to Te, dependence of size and quantum yield on heating time and spectra of ACYS-capped CdTe QDs. See DOI: 10.1039/b714990e

The Te disc electrode for cathodic stripping was prepared by sealing a Te rod (4 mm in diameter) in a glass tube. The generation of the Te precursor was carried out using an applied potential of −1.05 V in the electrolyte containing 2.0 mM Cd^{2+} and 4.8 mM MAA at pH 11 adjusted with 0.05 M NaOH solution. The reduction potential of $[Cd(MAA)_3]^{4-}$ was calculated to be −1.11 V from the equilibrium constant of $[Cd(MAA)_3]^{4-}$, thus this applied potential could avoid the deposition of Cd on the electrode (ESI†). The CdTe precursor could be easily formed due to the favorable thermodynamics[7] in the presence of MAA at pH 11, accompanied by a color change of the electrolyte from colorless to yellow and finally to dark brown. The amount of Te precursor was controlled by adjusting the charge consumed during cathodic stripping according to Faraday's law. Subsequently, the solution of CdTe precursor was heated in a water bath at 80 °C under stirring, and CdTe QDs were gradually crystallized. The size of the QDs could be controlled by changing the heating time, which was monitored by UV–Vis absorption with Peng's empirical equations.[8]

The molar ratio of Cd to Te greatly affected the luminescent behaviors of CdTe QDs at the same heating time, which could be measured by inductively coupled plasma (ESI†). The optimal molar ratio of Cd to Te occurred at 1 : 0.4, at which the obtained QDs showed the strongest PL emission. As shown in Fig. 1 and ESI† for MAA and ACYS stabilizers, all UV–Vis spectra showed well-resolved maximum absorption of the first electronic transition, indicating a sufficiently narrow size distribution of the QDs. The results were also confirmed from the PL spectra with a FWHM less than 44 nm.

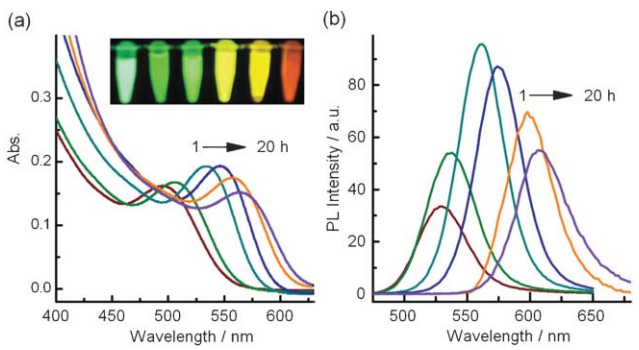

Fig. 1 UV–Vis absorption (a) and PL spectra (b) of MAA-capped CdTe QDs obtained at different heating times. The absorption peaks occur at 495, 506, 534, 547, 558 and 565 nm, and the PL emission peaks are at 530, 537, 562, 578, 598 and 609 nm (λ_{ex} = 388 nm) for the heating times of 1, 2, 6, 8, 14 and 20 h, respectively. The inset in (a) shows fluorescent photographs of as-prepared CdTe QDs under UV irradiation.

The fluorescent color under UV irradiation changed from green to yellow, orange and finally red with increasing heating time (inset in Fig. 1a). The red-shifts of the color, the absorption edge and the maximum PL emission wavelength indicated the growth of CdTe QDs during the heating treatment. The sizes of the QDs could be estimated from the UV–Vis absorption spectrum by Peng's empirical equations[8] to be from 2.0 to 3.5 nm. This indicated that the size of the QDs could be tuned simply by varying the heating time in the bath. The PL emission intensity also depended on the heating time (Fig. 1b). With the increase of heating time from 0.5 h to 6 h, the PL emission intensity increased due to the improvement of the crystallization and annealing effect of defects, and the maximum PL emission occurred at 6 h. This result was different from that observed previously[3c] and could be explained in terms of the mechanism of Ostwald ripening and defocusing.[9] However, further heating resulted in a decrease in PL emission intensity due to broad distribution and relatively small surface/volume ratio of the obtained QDs.

The UV–Vis absorption and PL spectra of QDs obtained from different synthesis batches showed close positions of absorption and emission peaks, and the same sharp shapes, indicating the similar size and good reproducibility of these as-prepared QDs.

With increasing heating time the QY of PL emission increased markedly. The changes were different for MAA- and ACYS-capped QDs (ESI†). The QY of MAA-capped CdTe QDs increased from 10.8% to 63.8% as the heating time was prolonged from 0.5 h to 8 h and then reached a maximum value of 77.3% at 20 h. The QY of ACYS-capped CdTe QDs also increased markedly from 12.1% at 0.5 h to a maximum value of 79.0% at 8 h. Further heating resulted in a slight decrease of QY. Such a remarkable QY is comparable with that reported for nonaqueous CdTe QDs (70%),[3] and much higher than those of CdTe QDs with aqueous synthesis.[2] The luminescence efficiency was stable during the storage of the CdTe crystallites at 4 °C over several months. These results indicate that the as-synthesized CdTe QDs have high QY and favorable stability. Thus, the proposed method to electrogenerate the precursor was efficient for the synthesis of highly luminescent CdTe QDs. The excellent photophysical behavior of QDs allowed fine-tuning to select discrete emission and excitation properties for biolabeling and imaging applications.

The morphology of the CdTe QDs was characterized with high-resolution transmission electron microscopy (HRTEM). It showed the lattice fringes of the particles with an average size of 3.2 nm (Fig. 2a), indicating a highly crystalline structure of CdTe. The average size was consistent with the result obtained from the UV–Vis absorption. The predominance of edged rhombohedral and tetrahedral crystallites seen from the HRTEM image indicated that the shape of the QDs could not be considered as near spherical.[4a] The Fourier transform pattern of the selected area further confirmed the short-range ordering crystallinity of these as-prepared QDs (Fig. 2b).

The heating time for obtaining CdTe QDs showed less influence on the interplanar distances. The HRTEM image showed interplanar distances of 3.57 and 2.13 Å in two directions (Fig. 2a), corresponding to those of 3.52 and 2.12 Å for CdTe in a hexagonal primitive-type structure (JCPDS 190193), which could not present in a cubic face-centered or orthorhombic primitive structure. The present CdTe QDs exhibited a structure different to that of cubic zinc blende described in previous reports.[4a,10] The dense accumulation of hexagonal primitive could be the structural origin of highly luminescent CdTe. As seen from Fig. 2c, the powder X-ray diffraction (XRD) spectrum showed a strong diffraction peak at the center of 25°. Several sharp diffraction peaks at the 2θ values of around 26.7° and 43.9° possibly came from the CdS phase in a hexagonal primitive type structure (JCPDS 010783), which was formed between MAA and the surface of the CdTe to result in a core–shell heterostructure, and usually found in mercapto-capped QDs.[11] In contrast, no phase of $Cd(OH)_2$, such as hexagonal primitive (JCPDS 730969), monoclinic end-centered (JCPDS 712137) or x-$Cd(OH)_2$ (JCPDS 120062), was observed in the powder XRD spectrum, indicating there was no hydroxide on the surface of the particles.

Information on the surface energy of the CdTe QDs could be obtained from their ECL behaviors. Fig. 3 shows the cyclic voltammograms (curve 1) and ECL curve (curve 2) of MAA-capped CdTe QDs solution on a glassy carbon electrode. Three small reduction peaks were observed at −0.43, −0.85 and −1.33 V, while two oxidation peaks appeared at −0.61 and +0.95 V, respectively. These cathodic peaks can be attributed to the reduction of Cd elements, CdTe and CdS phase, and atomic Te in the QDs.[12] The oxidation peaks resulted from the oxidation of the reduced state of Cd and the injection of holes in the $1S_h$ quantum-confined orbital of the CdTe core,[13] respectively.

Upon the potential scan a cathodic ECL peak was observed at −0.61 V, which was 1.24 V more positive than that of the cathodic

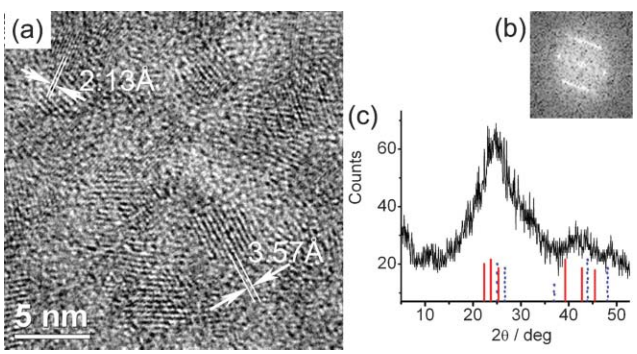

Fig. 2 HRTEM image (a), Fourier transform pattern of the selected area (b) and powder XRD spectrum (c) of MAA-capped CdTe QDs obtained on heating for 6 h.

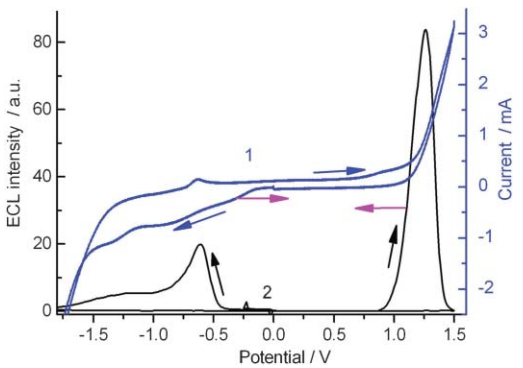

Fig. 3 Cyclic voltammograms (curve 1) and ECL curve (curve 2) of MAA-capped CdTe QDs solution on heating for 6 h on a glassy carbon electrode at a scan rate of 0.1 V s^{-1} in 0.1 M KCl as supporting electrolyte.

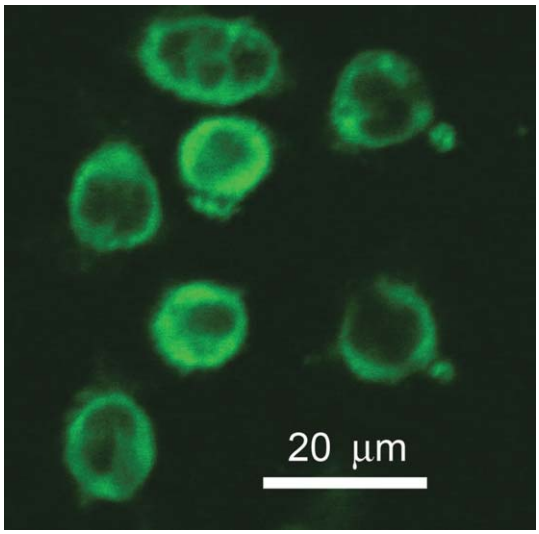

Fig. 4 Confocal micrograph of peritoneal macrophage from mouse incubated with CdTe QDs-labeled anti-MHC-II.

ECL emission of CdTe nanoparticles in organic media.[14] This emission cannot be explained by annihilation between redox species of QDs due to the absence of the oxidized species of QDs as electron acceptors. One possibility is that the emitter was produced by other oxidized species as coreactants from the supporting electrolyte or impurities.[12,14] Meanwhile, the ECL curve showed a strong anodic emission at +1.26 V. The anodic ECL emission can be attributed to an annihilation process between the holes-injected QDs and reduced species.[14] The electrochemical band gap between the two ECL peaks was 1.87 eV, which was less than that of 2.21 eV (562 nm) from PL emission peaks. This could be because the two ECL peaks are located at potentials inside the valence band edge for electron and hole injections into the surface traps of the particles.[14,15] The strong ECL behaviors further confirm the high luminescence and the potential ECL biosensing application of CdTe QDs synthesized with the electrogenerated precursor.

To verify the benefits of the as-prepared CdTe QDs, the MAA-capped CdTe QDs were employed to label a major histocompatibility complex class II (MHC-II) antibody for cell imaging. The avidin was conjugated to MAA-capped QDs *via* electrostatic self-assembly. After removing the excess avidin with an ultracentrifuge filter (MWCO 100 000 g mol^{-1}), the conjugates were coupled with anti-MHC-II *via* an avidin bridge[16] and then used for bioimaging the skeleton of mouse peritoneal macrophage. The nonspecific binding was effectively blocked by 1% bovine serum albumin (BSA). Fig. 4 shows the confocal micrograph of peritoneal macrophage from mouse incubated with CdTe QDs-labeled anti-MHC-II at 25 $\pm$ 1 °C, which is distributed in cytoplasm surrounding the nuclei. The CdTe QDs-labeled anti-MHC-II could specifically bind to cytoplasm immunogen of peritoneal macrophage. The accessibility of QDs labeled antibody to MHC-II in a cellular matrix illustrated the feasibility of using QDs for biological tagging and cell imaging.

In summary, an electrogenerated precursor is designed firstly for facile synthesis of highly luminescent CdTe QDs in aqueous solution with ecological safety, cost-efficiency, humidity insensitivity, and favorable reproducibility. The obtained CdTe QDs have good crystallizability, favorable monodispersity, high QY, strong anodic ECL emission and good stability. The present approach can be widely used in the preparation of CdTe capped with different surface stabilizers or other telluride QDs. Moreover, CdTe QDs can access cellular targets and stain the fine features such as the cell nucleolus; they have potential application as biolabels in sensitive biosensing and cell imaging.

This work was supported by the National Natural Science Foundation of China (No. 60571055, 20535010, 20521503, 20325518, 90713015) and China Postdoctoral Science Foundation (20060400914). We thank Fengli Bei (Nanjing University of Science & Technology) for HRTEM measurements.

Notes and references

1 (*a*) Y. Zheng, S. Gao and J. Y. Ying, *Adv. Mater.*, 2007, **19**, 376; (*b*) M. Bruchez, M. Moronne, P. Gin, S. Weiss and A. P. Alivisatos, *Science*, 1998, **281**, 2013.
2 (*a*) S. Kumar and T. Nann, *Chem. Commun.*, 2003, 2478; (*b*) C. B. Murray, D. J. Norris and M. G. Bawendi, *J. Am. Chem. Soc.*, 1993, **115**, 8706; (*c*) Y. A. Yang, H. M. Wu, K. R. Williams and Y. C. Cao, *Angew. Chem., Int. Ed.*, 2005, **44**, 6712.
3 (*a*) V. Sgobba, C. Schulz-Drost and D. M. Guldi, *Chem. Commun.*, 2007, 565; (*b*) H. Zhang, D. Wang, B. Yang and H. Möhwald, *J. Am. Chem. Soc.*, 2006, **128**, 10171; (*c*) M. Green, H. Harwood, C. Barrowman, P. Rahman, A. Eggeman, F. Festry, P. Dobsonb and T. Ng, *J. Mater. Chem.*, 2007, **17**, 1989.
4 (*a*) A. L. Rogach, L. Katsikas, A. Kornowski, D. Su, A. Eychmůller and H. Weller, *Ber. Bunsen-Ges. Phys. Chem.*, 1996, **100**, 1772; (*b*) T. Rajh, O. I. Mićić and A. J. Nozik, *J. Phys. Chem.*, 1993, **97**, 11999.
5 X. H. Li, I. S. Nandhakumar, T. Gabriel, G. S. Attard, M. L. Markham, D. C. Smith, J. J. Baumberg, K. Govender, P. O'Brien and D. Smyth-Boyle, *J. Mater. Chem.*, 2006, **16**, 3207.
6 A. W. Zhao, G. W. Meng, L. D. Zhang, T. Gao, S. H. Sun and Y. T. Pang, *Appl. Phys. A: Mater. Sci. Process.*, 2003, **76**, 537.
7 A. Shavel, N. Gaponik and A. Eychmüller, *J. Phys. Chem. B*, 2006, **110**, 19280.
8 W. W. Yu, L. Qu, W. Guo and X. Peng, *Chem. Mater.*, 2003, **15**, 2854.
9 X. Peng, J. Wickham and A. P. Alivisatos, *J. Am. Chem. Soc.*, 1998, **120**, 5343.
10 L. Li, H. F. Qian and J. C. Ren, *Chem. Commun.*, 2005, 528.
11 A. L. Rogach, *Mater. Sci. Eng., B*, 2000, **69–70**, 435.
12 A. J. Bard, Z. F. Ding and N. Myung, *Struct. Bonding*, 2005, **118**, 1.
13 I. A. Greene, F. Wu, J. Z. Zhang and S. Chen, *J. Phys. Chem. B*, 2003, **107**, 5733.
14 Y. Bae, N. Myung and A. J. Bard, *Nano Lett.*, 2004, **4**, 1153.
15 Z. Ding, B. M. Quinn, S. K. Haram, L. E. Pell, B. A. Korgel and A. J. Bard, *Science*, 2002, **296**, 1293.
16 E. R. Goldman, E. D. Balighian, H. Mattoussi, M. K. Kuno, J. M. Mauro, P. T. Tran and G. P. Anderson, *J. Am. Chem. Soc.*, 2002, **124**, 6378.

